Technische Universiteit Delft
Faculteit Elektrotechniek, Wiskunde en Informatica
Delft Institute of Applied Mathematics

Limit cycles in mass-spring systems with snap-through mechanisms

(Nederlandse titel: Geïsoleerde periodieke trillingen in massa-veer systemen met klikmechanismen)

Verslag ten behoeve van het
Delft Institute of Applied Mathematics
als onderdeel ter verkrijging

van de graad van

BACHELOR OF SCIENCE
in
TECHNISCHE WISKUNDE

door

LUCY SMEETS

Delft, Nederland
Juni 2019

BSc verslag TECHNISCHE WISKUNDE

"Limit cycles in mass-spring systems with snap-through mechanisms"

(Nederlandse titel: "Geïsoleerde periodieke trillingen in massa-veer systemen met klikmechanismen")

LUCY SMEETS

Technische Universiteit Delft

Begeleider

Dr. ir. W.T. van Horssen

Overige commissieleden

Dr. ir. F. J. Vermolen

Dr. B. van den Dries

Juni, 2019

Delft

Abstract

Mass-spring systems are commonly used in structural components. Understanding their characteristics and pitfalls is an important issue, combining physics and mathematics to prevent such systems from resonating and causing structures to weaken or collapse. This way, suitable solutions can be found such as the use of dampers with the right characteristics.

In this paper we focus on such systems, in particular with a snap-through mechanism. Their dynamical behaviour and the influence of a small disturbance on the mechanism, such as a wind force, are analyzed. A behavioral model is set up to which Melnikov's Method is applied, in order to analyze the behaviour numerically. The latter is done using the Trapezoidal method.

Contents

1: Frequently used notations

Notation	Description	Dimension
x	Vertical displacement	m
y	Vertical velocity	$\frac{m}{s}$
l	Initial spring length	m
l_0	Original spring length	m
m	Mass of the particle	kg
k	Vertical spring constant	$\frac{kg}{s^2}$
k_1	Horizontal spring constant	$\frac{kg}{s^2}$
$\varepsilon = \frac{\rho d \beta \zeta}{2m}$	Wind force	$\frac{m \cdot kg}{s^2}$
$\beta = \sqrt{\frac{3\gamma l^2}{\zeta}}$	Tool to make variables dimensionless	s
$\bar{x}$	Dimensionless version of vertical displacement	
$\bar{y}$	Dimensionless version of vertical velocity	
$\mu = \frac{l_0}{l}$	Ratio of original and initial spring length	
$\bar{k} = \frac{k\beta^2}{m}$	Dimensionless version of vertical spring constant	
$\bar{k_1} = \frac{k_1\beta^2}{m}$	Dimensionless version of horizontal spring constant	

2: Introduction

Figure 2.1 shows a mass-spring set-up with a snap-through mechanism. It consists of a mass attached to three springs: two horizontal springs with spring constant k_1, and a vertical spring with spring constant k. The original length of the horizontal springs is denoted by l_0, and their initial length when stretched out or pressed in by l. The vertical spring is in its initial state neither pressed in nor stretched out. The problem can be divided into two cases: $l \geq l_0$ (the horizontal springs are stretched out or of original length) and $l < l_0$ (pressed in).

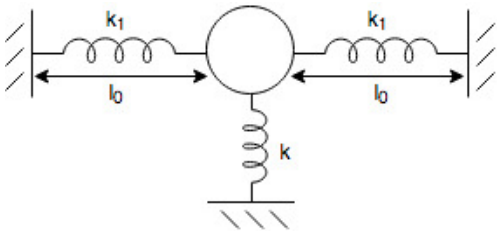

Figure 2.1: The mass-spring set-up in its original state, where $l = l_0$.

For simplicity, the mass is assumed to move in vertical direction only. This means that the horizontal springs will always be of the same length. Therefore, it is important to know the force of these springs on the mass in vertical direction. The displacement is a function of time, but for clarity, it is denoted as x. When the displacement x equals 0, just like in Figure 2.1, the force for each horizontal spring is equal to

$$F_{spring} = -k_1 \left(l - l_0\right), \tag{2.1}$$

with $k_1 > 0$. This equation holds for $l < l_0$, $l = l_0$ and $l > l_0$. The minus sign makes sure the forces point in the correct direction. When the springs are pressed in, such that $l < l_0$, $l - l_0$ will be negative, but the force will be positive, because the springs want to push out. The same reasoning holds for the other cases.
When the mass has a displacement of $x = x$ with an angle of θ with respect to the horizontal axis, the length of the spring becomes $\sqrt{l^2 + x^2}$ (see Figure 2.2).
This results in the following force in each horizontal spring:

$$F_{spring} = -k_1 \left(\sqrt{l^2 + x^2} - l_0\right), \tag{2.2}$$

and in vertical direction it gives

$$F_{spring,x} = \sin\theta \cdot -k_1 \left(\sqrt{l^2 + x^2} - l_0\right). \tag{2.3}$$

Since $\sin\theta$ can also be written as $\frac{x}{\sqrt{l^2+x^2}}$, the final force in vertical direction for each horizontal spring is as follows:

$$F_{spring,x} = -k_1 \cdot x \left(1 - \frac{l_0}{\sqrt{l^2 + x^2}}\right). \tag{2.4}$$

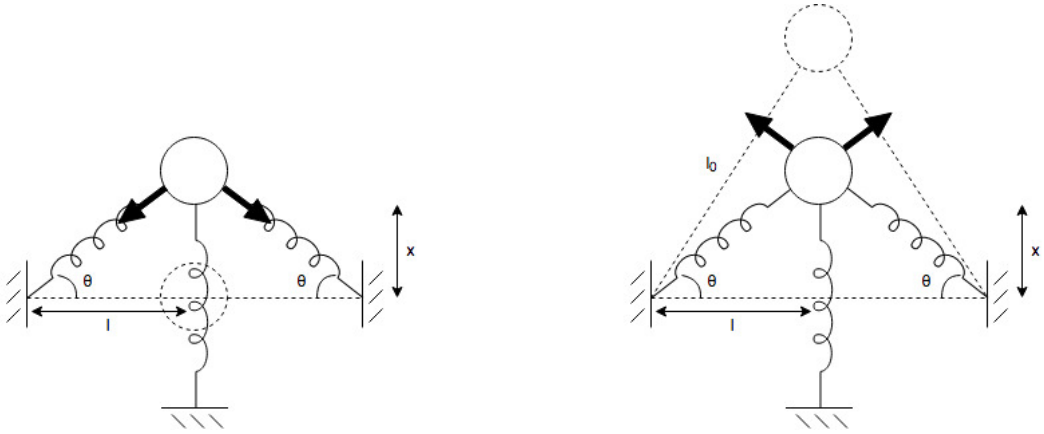

(a) $l \geq l_0$ (b) $l < l_0$

Figure 2.2: The mass-spring set-up for stretched out (a) and pressed in (b) springs. The arrows indicate the forces acting on the mass due to the non-vertical springs.

The total force of both horizontal springs on the mass will be (2.4) with a factor of 2. For the vertical spring, it is assumed that no force is acting on the mass at $x = 0$. The final equation of motion for the mass according to Newton's second law of motion will be

$$m\ddot{x} = -kx + 2k_1 x \left(\frac{l_0}{\sqrt{l^2 + x^2}} - 1 \right) + \text{"other external forces"}, \tag{2.5}$$

with $k > 0$ and m the weight of the mass. In (2.5), $-kx$ denotes the force of the vertical spring and has a minus sign to make sure it points in the right direction. The "other external forces" will be set to zero for now, but will represent wind forces later on.

3: Mathematical model

Equation (2.5), found in Chapter 2, contains a lot of parameters. To reduce this amount, the variables $\bar{x}$ and $\bar{t}$ are introduced as dimensionless versions of x and t:

$$\begin{cases} x = l\bar{x}, \\ t = \beta\bar{t}. \end{cases} \tag{3.1}$$

Substituting these dimensionless variables into (2.5) results in the following:

$$\ddot{\bar{x}} + \bar{k}\bar{x} - 2\bar{k_1}\bar{x}\left(\frac{\mu}{\sqrt{1+\bar{x}^2}} - 1\right) = \text{"other external forces"}, \tag{3.2}$$

where $\bar{k} = \frac{k\beta^2}{m}$, $\bar{k_1} = \frac{k_1\beta^2}{m}$ and $\mu = \frac{l_0}{l}$. First, we study the case without any external forces. Later on, we will add a wind force.

3.1 No external forces

We study the equation with no external forces acting on the mass:

$$\ddot{\bar{x}} + \bar{k}\bar{x} - 2\bar{k_1}\bar{x}\left(\frac{\mu}{\sqrt{1+\bar{x}^2}} - 1\right) = 0. \tag{3.3}$$

Multiplying (3.3) with $\dot{\bar{x}}$ gives the first integral:

$$\mathrm{F}(\bar{x}, \dot{\bar{x}}) = \frac{1}{2}\dot{\bar{x}}^2 + \frac{1}{2}\bar{k}\bar{x}^2 - \bar{k_1}\left(2\mu\sqrt{1+\bar{x}^2} - \bar{x}^2\right) = \text{constant}. \tag{3.4}$$

The Taylor series of (3.4) is calculated in the equilibrium points of the model to use Morse's Theorem [5] to get the phase portraits of the different cases. In the case where the horizontal springs are stretched out, so where $\mu < 1$, there is one equilibrium point at $(\bar{x}, \dot{\bar{x}}) = (0, 0)$. When $\mu > 1$, there are two additional equilibrium points at $\left(\pm\sqrt{\frac{\mu^2}{(1+\frac{\bar{k}}{2\bar{k_1}})^2} - 1}, 0\right)$.
Morse's Theorem needs only the constant and quadratic terms of the Taylor series. The Taylor series around $(0, 0)$ gives

$$-\frac{2\bar{k_1}}{\bar{k}}\mu + \frac{1}{2}\left(1 - \frac{2\bar{k_1}}{\bar{k}}(\mu - 1)\right)\bar{x}^2 + \frac{1}{2}\dot{\bar{x}}^2. \tag{3.5}$$

According to Morse's Theorem, the phase portrait has a saddlepoint in $(0, 0)$ when $\mu > 1 + \frac{\bar{k}}{2\bar{k_1}}$ and a centerpoint when $\mu < 1 + \frac{\bar{k}}{2\bar{k_1}}$. This means that in the case that the horizontal springs are stretched out, there is always a centerpoint at $(0, 0)$. When the springs are pressed in, the phase portrait has a saddlepoint at $(0, 0)$, but only when $\mu > 1 + \frac{\bar{k}}{2\bar{k_1}}$. So if the springs are pressed in,

but $1 < \mu < 1 + \frac{\bar{k}}{2\bar{k_1}}$ and $\bar{k}$ is big with respect to $\bar{k_1}$, there is still a centerpoint at $(0, 0)$.
The Taylor series around the other equilibrium points with regard to Morse's Theorem gives

$$\begin{aligned}
\mathrm{F}(\bar{x}, \dot{\bar{x}}) &= \frac{1}{2}\dot{\bar{x}}^2 + \frac{1}{2}\bar{k}\bar{x}^2 - \bar{k_1}\left(2\mu\sqrt{1+\bar{x}^2} - \bar{x}^2\right) \\
&= \mathrm{F}\left(\pm\sqrt{\frac{\mu^2}{(1+\frac{\bar{k}}{2\bar{k_1}})^2} - 1, 0}\right) + \frac{1}{2}\mathrm{F}_{\bar{x}\bar{x}}\left(\pm\sqrt{\frac{\mu^2}{(1+\frac{\bar{k}}{2\bar{k_1}})^2} - 1, 0}\right)\left(\bar{x} - \sqrt{\frac{\mu^2}{(1+\frac{\bar{k}}{2\bar{k_1}})^2} - 1}\right)^2 \\
&\quad + \frac{1}{2}\mathrm{F}_{\dot{\bar{x}}\dot{\bar{x}}}\left(\pm\sqrt{\frac{\mu^2}{(1+\frac{\bar{k}}{2\bar{k_1}})^2} - 1, 0}\right)(\dot{\bar{x}} - 0)^2 \\
&= \frac{1}{2}\left(\frac{\mu^2}{(1+\frac{\bar{k}}{2\bar{k_1}})^2} - 1\right) - \frac{1}{2}\frac{2\bar{k_1}}{\bar{k}}\left(\frac{2\mu^2}{1+\frac{\bar{k}}{2\bar{k_1}}} - \frac{\mu^2}{(1+\frac{\bar{k}}{2\bar{k_1}})^2} + 1\right) \\
&\quad + \frac{1}{2}\left(1 - \frac{2\bar{k_1}}{\bar{k}}\left(\frac{(1+\frac{\bar{k}}{2\bar{k_1}})^3}{\mu^2} - 1\right)\right)\bar{x}^2 + \frac{1}{2}\dot{\bar{x}}^2.
\end{aligned}$$

Linear terms are automatically eliminated because of the Taylor expansion. Following from Morse's Theorem, there are two centerpoints at both equilibrium points when $\mu > 1 + \frac{\bar{k}}{2\bar{k_1}}$. The results for $\bar{k_1} > 0$ are shown in Figure 3.1. The case when $\bar{k_1} = 0$, which means there are no horizontal springs, gives a phase portrait similar to Figure 3.1(a).

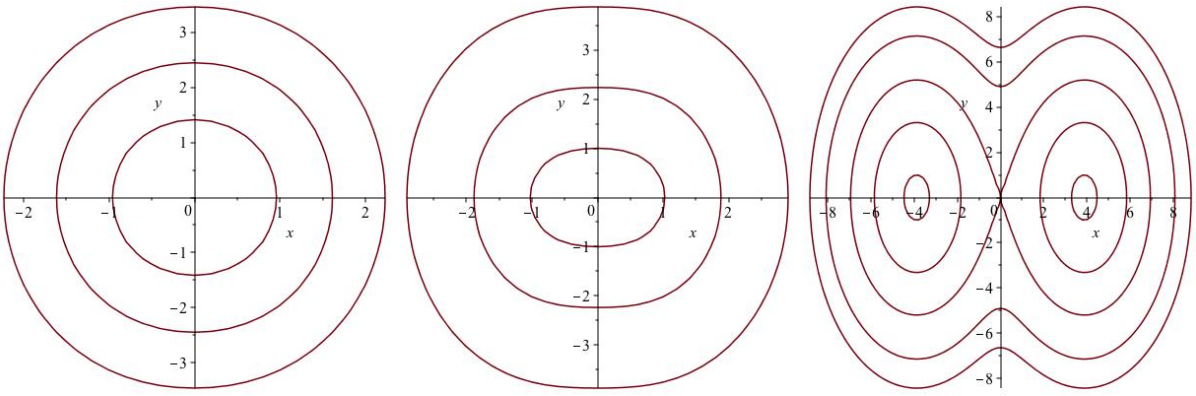

(a) $\mu \leq 1$ (b) $1 < \mu \leq 1 + \frac{\bar{k}}{2\bar{k_1}}$ (c) $\mu > 1 + \frac{\bar{k}}{2\bar{k_1}}$

Figure 3.1: Phase portraits for different ratios of the spring lengths and constants.

3.2 External force: wind

Now a wind force is added to the equation of motion. Figure 3.2 shows a cross section of the mass with the drag (D) and lift (L) forces as a result of the wind (v_0) acting on it.

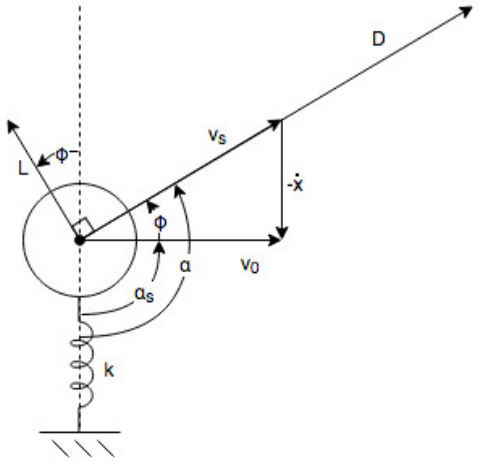

Figure 3.2: Wind force acting on a cross section of the mass.

Again, only the vertical displacement is important. This results in the following equation of motion:

$$m\ddot{x} + kx - 2k_1 x\left(\frac{l_0}{\sqrt{l^2+x^2}} - 1\right) = D\sin\phi + L\cos\phi, \tag{3.6}$$

with D and L defined as follows [4]:

$$D = \frac{\rho d c^D(\alpha)}{2} v_s^2, \tag{3.7}$$

$$L = \frac{\rho d c^L(\alpha)}{2} v_s^2. \tag{3.8}$$

Here, d denotes the diameter of the mass, ρ the air density, c^D and c^L the drag and lift coefficients respectively, v_s the wind force in the same direction as the drag, and α the angle between v_s and the symmetry-axis (the dotted line). The drag and lift coefficients are approximated by (see [4]):

$$c^D(\alpha) = c_0^D, \tag{3.9}$$

$$c^L(\alpha) = c_1^L(\alpha - \alpha_0) + c_3^L(\alpha - \alpha_0)^3. \tag{3.10}$$

Furthermore, the following is known:

$$v_s^2 = \dot{x}^2 + v_0^2, \quad \cos\phi = \frac{v_0}{v_s}, \quad \sin\phi = -\frac{\dot{x}}{v_s}, \quad \tan\phi = -\frac{\dot{x}}{v_0}, \quad \alpha = \alpha_s + \phi. \tag{3.11}$$

By expressing all expressions in $\frac{\dot{x}}{v_0}$, the right-hand side of (3.6) becomes

$$\frac{\rho d}{2}\left(-c_0^D v_0^2\sqrt{1+\left(\frac{\dot{x}}{v_0}\right)^2}\frac{\dot{x}}{v_0} + c_1^L \arctan\left(\frac{-\dot{x}}{v_0}\right) v_0^2\sqrt{1+\left(\frac{\dot{x}}{v_0}\right)^2} + c_3^L \arctan^3\left(\frac{-\dot{x}}{v_0}\right) v_0^2\sqrt{1+\left(\frac{\dot{x}}{v_0}\right)^2}\right). \tag{3.12}$$

The Taylor series of this equation around $\frac{\dot{x}}{v_0} = 0$ is

$$\frac{\rho d}{2}\left(-v_0\left(c_0^D + c_1^L\right)\dot{x} - \left(\frac{1}{2}c_0^D + \frac{1}{6}c_1^L + c_3^L\right)\frac{\dot{x}^3}{v_0}\right). \tag{3.13}$$

Eventually, the equation of motion of the particle when taking wind forces into account is found:

$$m\ddot{x} + kx - 2k_1 x\left(\frac{l_0}{\sqrt{l^2 + x^2}} - 1\right) = \frac{\rho d}{2}\left(\zeta\dot{x} - \gamma\dot{x}^3\right). \tag{3.14}$$

Here, $\zeta = -v_0\left(c_0^D + c_1^L\right)$ and $\gamma = \left(\frac{1}{2}c_0^D + \frac{1}{6}c_1^L + c_3^L\right)\frac{1}{v_0}$. Again, using $x = l\bar{x}$ and $t = \beta\bar{t}$ to make x and t dimensionless variables, a new equation of motion with less variables is found:

$$\ddot{\bar{x}} + \bar{k}\bar{x} - 2\bar{k_1}\bar{x}\left(\frac{\mu}{\sqrt{1 + \bar{x}^2}} - 1\right) = \varepsilon\left(\dot{\bar{x}} - \frac{1}{3}\dot{\bar{x}}^3\right). \tag{3.15}$$

Here are $\bar{k} = \frac{k\beta^2}{m}$, $\bar{k_1} = \frac{k_1\beta^2}{m}$, $\mu = \frac{l_0}{l}$, $\beta^2 = \frac{3\gamma l^2}{\zeta}$ and $\varepsilon = \frac{\rho d\beta\zeta}{2m}$, with $0 < \varepsilon \ll 1$.

4: Problem

From now on, the focus will be on the problem regarding a small disturbance (a wind force) working on the mass. How many periodic solutions exist for a small disturbance like this and what is their stability? For this, we consider the equation of motion (4.1).

$$\ddot{\bar{x}} + \bar{k}\bar{x} - 2\bar{k_1}\bar{x}\left(\frac{\mu}{\sqrt{1+\bar{x}^2}} - 1\right) = \varepsilon\left(\dot{\bar{x}} - \frac{1}{3}\dot{\bar{x}}^3\right). \tag{4.1}$$

The problem can be categorized in four subproblems:

1. $\bar{k_1} = 0$
2. $\bar{k} = 0$, $0 < \mu \leq 1$
3. $\bar{k} = 0$, $\mu > 1$
4. $\bar{k_1}$, $\bar{k} \neq 0$

This division is made based on increasing difficulty. Subproblem 1 describes a problem with a linear oscillator, as the other subproblems are non-linear. As seen in Chapter 3, subproblem 2 studies stretched out springs and has only one equilibrium point, while subproblem 3 studies pressed in springs and has three equilibrium points. It is important to distinguish cases based on these characteristics. Lastly, subproblem 4 is the most difficult one since it describes both the linear and non-linear oscillator. It is further split into three categories as seen before: $0 < \mu < 1$, $1 < \mu < 1 + \frac{\bar{k}}{2\bar{k_1}}$ and $\mu > 1 + \frac{\bar{k}}{2\bar{k_1}}$. The first category studies the system with stretched out springs, while the other two study a pressed in system. When pressed in, the division is made based on the amount of equilibrium points again (one and three respectively).

In this paper, only subproblems 1 to 3 are analyzed. Therefore, a study of the needed theory is presented next.

5: Theory

To be able to study the problem, some theory is needed. The theory behind Melnikov's Method (see [3]) normally covers the general situation where $\mathbf{x} \in \mathbb{R}^n$. Since this problem only uses two-dimensional vectors, this chapter will limit the theory to $\mathbf{x} \in \mathbb{R}^2$. Later on, the theory will be applied to each of the subproblems as described in Chapter 4. Melnikov's Method can be used to show the existence of limit cycles of perturbed planar systems of the following form:

$$\ddot{x} + \frac{\mathrm{d}V}{\mathrm{d}x}(x) = \varepsilon f(x, \dot{x}). \tag{5.1}$$

Rewriting (5.1) as a system of differential equations gives the following:

$$\begin{cases} \dot{x} = y, \\ \dot{y} = -\frac{\mathrm{d}V}{\mathrm{d}x}(x) + \varepsilon f(x, y). \end{cases} \tag{5.2}$$

When $\varepsilon = 0$, the Hamiltonian of (5.1) is given by:

$$\mathrm{H}(x, y) = \frac{1}{2}y^2 + V(x). \tag{5.3}$$

Knowing this, (5.2) can be rewritten as follows:

$$\begin{cases} \dot{x} = \frac{\partial \mathrm{H}}{\partial y}, \\ \dot{y} = -\frac{\partial \mathrm{H}}{\partial x} + \varepsilon f(x, y). \end{cases} \tag{5.4}$$

To use Melnikov's Method, $\frac{\mathrm{dH}}{\mathrm{d}t}$ needs to be known. The following can be concluded, using (5.4):

$$\begin{aligned} \frac{\mathrm{dH}}{\mathrm{d}t} &= \frac{\partial \mathrm{H}}{\partial x}\frac{\mathrm{d}x}{\mathrm{d}t} + \frac{\partial \mathrm{H}}{\partial y}\frac{\mathrm{d}y}{\mathrm{d}t} && (5.5) \\ &= \mathrm{H}_x\mathrm{H}_y + \mathrm{H}_y \cdot (-\mathrm{H}_x + \varepsilon f(x, y)) && (5.6) \\ &= \varepsilon \mathrm{H}_y f(x, y). && (5.7) \end{aligned}$$

Let $\mathrm{H}(x, y) = h$ be a closed orbit in the (x, y)-plane and let T_h be the period of this orbit. Now, we get the Melnikov function:

$$\int_0^{\mathrm{T}_h} \frac{\mathrm{dH}}{\mathrm{d}s}(x(s), y(s))ds = \varepsilon \int_0^{\mathrm{T}_h} y(s) \cdot f(x(s), y(s))ds. \tag{5.8}$$

The left-hand side of (5.8) can also be written as $\mathrm{H}(x(\mathrm{T}_h), y(\mathrm{T}_h)) - \mathrm{H}(x(0), y(0))$. When this equation equals zero, it depicts a periodic solution of the problem with $\varepsilon \neq 0$. So, zeros of $\varepsilon \int_0^{\mathrm{T}_h} y(s) \cdot f(x(s), y(s))ds$ determine periodic solutions of this problem. See for an example Figure 5.1.

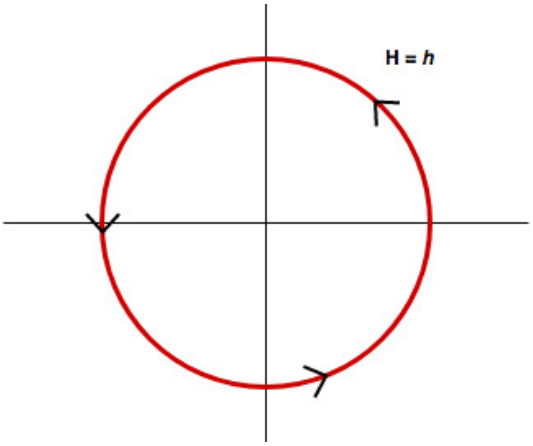

Figure 5.1: A periodic solution.

In Figure 5.1, it is clear that the orbit is symmetric in the x-axis. This is a result of $\mathrm{H}(x, y)$ being equal to both h and $\frac{1}{2}y^2 + V(x)$. Now consider the following integral (part of (5.8)).

$$\mathrm{M}(h) = \int_0^{\mathrm{T}_h} y(s) \cdot f(x(s), y(s))ds. \tag{5.9}$$

Using the symmetry in the x-axis, (5.9) can be simplified to the following:

$$\mathrm{M}(h) = 2 \cdot \int_0^{\frac{1}{2}\mathrm{T}_h} y(s) \cdot f(x(s), y(s))ds. \tag{5.10}$$

Figure 5.2 shows the part of the orbit that (5.10) covers.

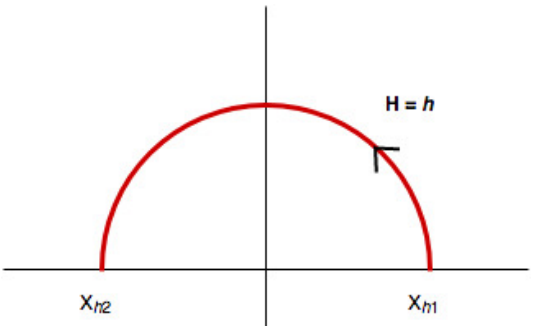

Figure 5.2: The first half of a periodic solution, from X_{h1} to X_{h2}.

To determine the zeros of (5.10), it should be an integral of x or y instead of t. It turns out that it is most convenient to make it an integral of x, with X_{h1} as the $\bar{x}$-coordinate of the curve at $t = 0$ (see Figure 5.2) and X_{h2} as the $\bar{x}$-coordinate at $t = \frac{1}{2}\mathrm{T}_h$:

$$\mathrm{M}(h) = 2 \cdot \int_{\mathrm{X}_{h1}}^{\mathrm{X}_{h2}} y(s) \cdot f(x(s), y(s))ds \tag{5.11}$$

$$= 2 \cdot \int_{\mathrm{X}_{h1}}^{\mathrm{X}_{h2}} y(s) \cdot f(x(s), y(s)) \frac{dx}{\frac{dx}{ds}} \tag{5.12}$$

$$= 2 \cdot \int_{\mathrm{X}_{h1}}^{\mathrm{X}_{h2}} f(x(s), y(s))dx. \tag{5.13}$$

Equation (5.13) holds because of $\frac{dx}{ds} = y(s)$, according to (5.2). This integral concludes the general part of the theory.
This theory will be applied to the subproblems of this paper stated in Chapter 4, with equation of motion (4.1). The zeros of (5.13) will represent the limit cycles of each subproblem respectively. Using the book of Perko [3], the stability of these limit cycles will be investigated.

6: Analysis

In Chapter 3, we found phase portraits for different subproblems. It is interesting to see what will happen to them when adding a little distortion. In order to do so, Melnikov's Method will be applied to the equation of motion:

$$\ddot{\bar{x}} + \bar{k}\bar{x} - 2\bar{k_1}\bar{x}\left(\frac{\mu}{\sqrt{1+\bar{x}^2}} - 1\right) = \varepsilon\left(\dot{\bar{x}} - \frac{1}{3}\dot{\bar{x}}^3\right). \tag{6.1}$$

In this paper, we will apply this method to subproblems 1 to 3. An analysis on the complete equation of motion (subproblem 4) can be made in further research.

6.1 Linear oscillator

First, we consider subproblem 1, as described in Chapter 4. This is the case where $\bar{k_1} = 0$, which means that there are no horizontal springs, but only one vertical spring attached to the mass (see Figure 6.1).

Figure 6.1: The mass-spring set-up with $\bar{k_1} = 0$.

This means the following equation, which describes a linear oscillator, has to be studied:

$$\ddot{\bar{x}} + \bar{k}\bar{x} = \varepsilon\left(\dot{\bar{x}} - \frac{1}{3}\dot{\bar{x}}^3\right). \tag{6.2}$$

According to Chapter 5, the Hamiltonian gives $\mathrm{H}(\bar{x}, \bar{y}) = \frac{1}{2}\bar{y}^2 + \frac{1}{2}\bar{k}\bar{x}^2 = h$ and we get the following system of differential equations:

$$\mathbf{F}(\bar{x}, \bar{y}) = \begin{cases} \dot{\bar{x}} = \bar{y}, \\ \dot{\bar{y}} = -\bar{k}\bar{x} + \varepsilon\left(\bar{y} - \frac{1}{3}\bar{y}^3\right). \end{cases} \tag{6.3}$$

When no distortion is added, meaning $\varepsilon = 0$, (6.2) has the following solutions:

$$\begin{cases} \dot{\bar{x}}(t) = c_1\cos\left(\sqrt{\bar{k}}t\right) + c_2\sin\left(\sqrt{\bar{k}}t\right) = A\sin\left(\sqrt{\bar{k}}t + \alpha\right), \\ \dot{\bar{y}}(t) = -c_1\sqrt{\bar{k}}\sin\left(\sqrt{\bar{k}}t\right) + c_2\sqrt{\bar{k}}\cos\left(\sqrt{\bar{k}}t\right) = A\sqrt{\bar{k}}\cos\left(\sqrt{\bar{k}}t + \alpha\right). \end{cases} \tag{6.4}$$

From (6.4), it follows that the period equals $\mathrm{T}_h = \frac{2\pi}{\sqrt{\bar{k}}}$. In combination with the Hamiltonian, it also follows that $A = \sqrt{\frac{2h}{\bar{k}}}$. Taking $\alpha = 0$, gives the curve of Figure 6.2, starting at (0,1). The curve is oriented clockwise without loss of generality, because $\dot{\bar{y}} < 0$ in (6.3) for $\bar{y} = 0$ and $\bar{x} > 0$.

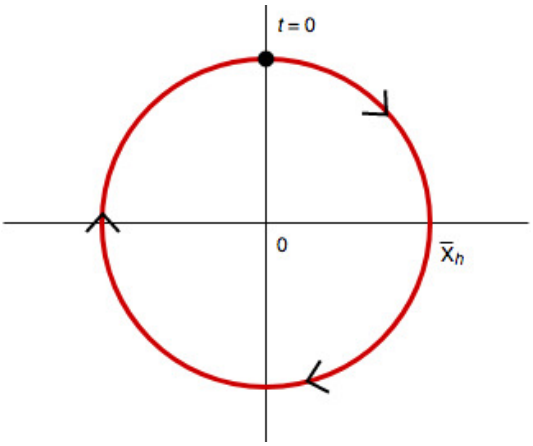

Figure 6.2: A periodic solution of the problem with $\bar{k_1} = 0$.

The integral from (5.9) is studied for this case:

$$\mathrm{M}(h) = \int_0^{\mathrm{T}_h} \bar{y}(s) \cdot f(\bar{x}(s), \bar{y}(s)) ds \tag{6.5}$$

$$= \int_0^{\frac{2\pi}{\sqrt{\bar{k}}}} \sqrt{2h}\cos\left(\sqrt{\bar{k}}t\right) \cdot \left(\sqrt{2h}\cos\left(\sqrt{\bar{k}}t\right) - \frac{1}{3}\left(\sqrt{2h}\cos\left(\sqrt{\bar{k}}t\right)\right)^3\right) dt \tag{6.6}$$

$$= \int_0^{\frac{2\pi}{\sqrt{\bar{k}}}} 2h\cos^2(\sqrt{\bar{k}}t)dt - \frac{1}{3}\int_0^{\frac{2\pi}{\sqrt{\bar{k}}}} 4h^2\cos^4(\sqrt{\bar{k}}t)dt \tag{6.7}$$

$$= \frac{2\pi h}{\sqrt{\bar{k}}} - \frac{1}{3}\frac{3\pi h^2}{\sqrt{\bar{k}}} \tag{6.8}$$

$$= \frac{\pi h(2-h)}{\sqrt{\bar{k}}}. \tag{6.9}$$

As described in Chapter 5, zeros of $\mathrm{M}(h)$ depict periodic solutions of the problem. $\mathrm{M}(h) = 0$ is true when $h = 2$ (and $h = 0$). It follows from the Hamiltonian and $\bar{\mathrm{X}}_h = h$ that $h = \frac{2}{\bar{k}}$ and thus $\bar{k} = 1$.

To study the stability of this solution, the Corollary of paragraph 3.4 [3] is used. It says that the periodic solution $\gamma(t)$ of (6.3) is a stable limit cycle if $\int_0^{\mathrm{T}} \nabla \cdot \mathbf{F}(\gamma(t))dt < 0$, with $\mathrm{T} = \frac{2\pi}{\sqrt{\bar{k}}}$ the period of the limit cycle.

In this case, $\gamma(t) = \left(2\sin\left(\sqrt{\bar{k}}t\right), 2\cos\left(\sqrt{\bar{k}}t\right)\right)^\top$ and $\nabla \cdot \mathbf{F}(\bar{x}, \bar{y}) = \varepsilon\left(1 - \bar{y}^2\right)$, so $\nabla\mathbf{F}(\gamma(t)) = \varepsilon\left(1 - 4\cos^2(\sqrt{\bar{k}}t)\right)$. This gives the following integral:

$$\int_0^{\mathrm{T}} \nabla \cdot \mathbf{F}(\gamma(t))dt = \varepsilon \int_0^{\frac{2\pi}{\sqrt{\bar{k}}}} 1 - 4\cos^2(\sqrt{\bar{k}}t)dt = \frac{-2\pi\varepsilon}{\sqrt{\bar{k}}} < 0, \tag{6.10}$$

since $0 < \varepsilon \ll 1$ and $\bar{k} > 0$. According to the Corollary, the limit cycle is stable. This result is depicted in Figure 6.3.

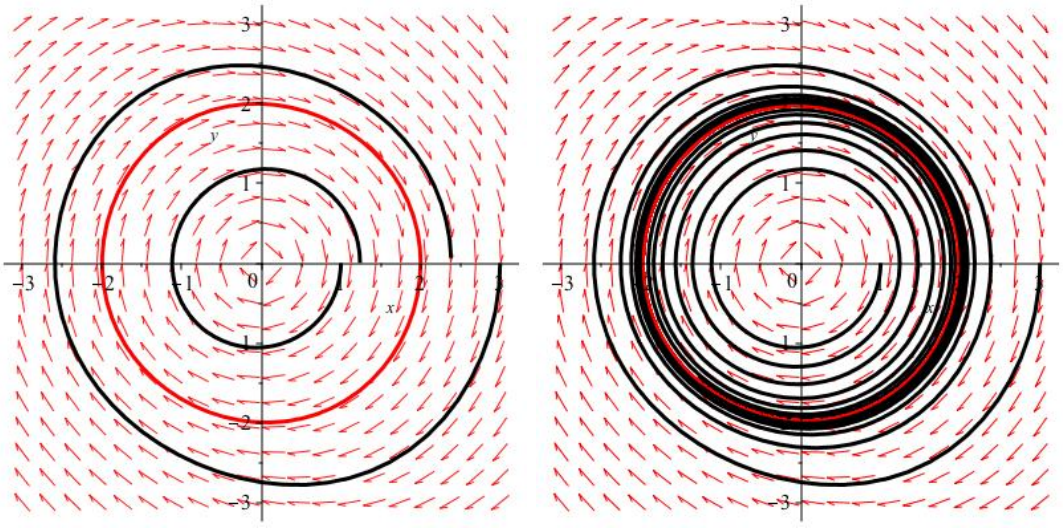

(a) Curves starting at $(\bar{x}, \bar{y}) = (1,0), (2,0), (3,0)$ with $0 \leq t \leq 2\pi$.

(b) Curves starting at $(\bar{x}, \bar{y}) = (1,0), (2,0), (3,0)$ and ending at the limit cycle.

Figure 6.3: Phase portraits of (6.3) with the stable limit cycle of radius 2 (red) and curves at the interior and exterior of the solution, moving towards the limit cycle.

To verify these results, a MATLAB script is written. This can be found in Appendix A. It uses the Trapezoidal integration method on Equation 6.6. The result is shown in Figure 6.4. It follows that indeed $\mathrm{M}(h) = 0$ for $h = 0$ and $h = 2$.

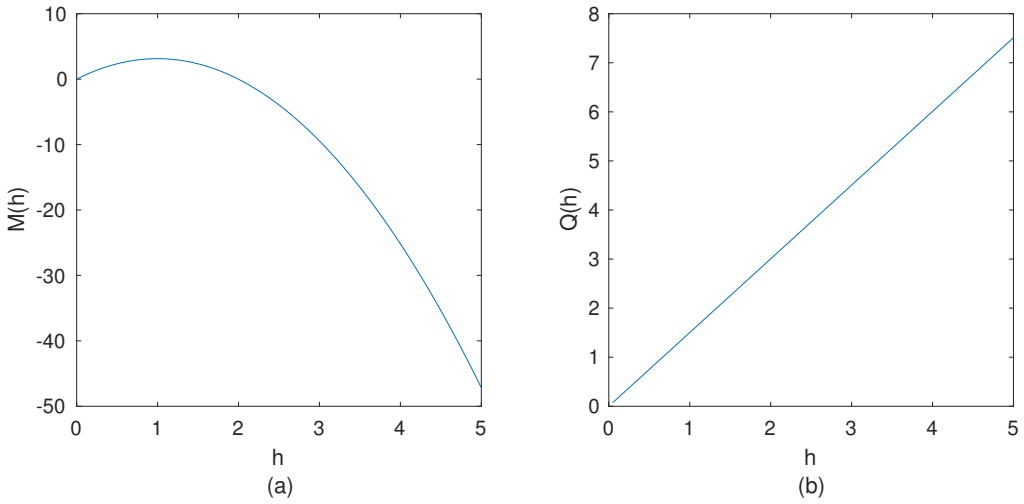

Figure 6.4: Value of (6.6) and $\mathrm{Q}(h)$ for different values of h with $\bar{k} = 1$ and $\bar{k_1} = 0$.

6.2 Non-linear oscillator

Both subproblems 2 and 3, as specified in Chapter 4, describe a non-linear oscillator ($\bar{k} = 0$). This means that there is no vertical spring, but only the two horizontal springs attached to the mass (see Figure 6.5). We distinguish two cases; the springs are either stretched out ($0 < \mu \leq 1$) or pressed in ($\mu > 1$).

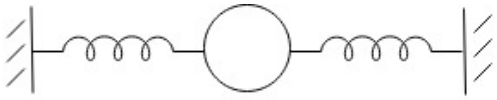

Figure 6.5: The mass-spring set-up with $\bar{k} = 0$.

6.2.1 Stretched out springs

First we look at subproblem 2, with $0 < \mu \leq 1$, which means that the springs are stretched out. The following equation is to be studied:

$$\ddot{\bar{x}} - 2\bar{k_1}\bar{x}\left(\frac{\mu}{\sqrt{1+\bar{x}^2}} - 1\right) = \varepsilon\left(\dot{\bar{x}} - \frac{1}{3}\dot{\bar{x}}^3\right). \tag{6.11}$$

Applying the theory of Chapter 5, this results in $\mathrm{H}(\bar{x}, \bar{y}) = \frac{1}{2}\bar{y}^2 - \bar{k_1}\left(2\mu\sqrt{1+\bar{x}^2} - \bar{x}^2\right) = h$ and the following system of differential equations:

$$\mathbf{F}(\bar{x}, \bar{y}) = \begin{cases} \dot{\bar{x}} = \bar{y}, \\ \dot{\bar{y}} = 2\bar{k_1}\bar{x}\left(\frac{\mu}{\sqrt{1+\bar{x}^2}} - 1\right) + \varepsilon\left(\bar{y} - \frac{1}{3}\bar{y}^3\right). \end{cases} \tag{6.12}$$

Also, we find the terms

$$f(\bar{x}, \bar{y}) = \bar{y} - \frac{1}{3}\bar{y}^3, \quad \frac{\mathrm{d}V}{\mathrm{d}\bar{x}}(\bar{x}) = -2\bar{k_1}\bar{x}\left(\frac{\mu}{\sqrt{1+\bar{x}^2}} - 1\right). \tag{6.13}$$

This results in $V(\bar{x}) = -\bar{k_1}\left(2\mu\sqrt{1+\bar{x}^2} - \bar{x}^2\right)$. The Hamiltonian in this case is described by $\mathrm{H}(\bar{x}, \bar{y}) = \frac{1}{2}\bar{y}^2 + V(\bar{x})$. Let $\mathrm{H}(\bar{x}, \bar{y}) = h$ now be a closed orbit in the $(\bar{x}, \bar{y})$-plane. It is clear that $f(\bar{x}, \bar{y})$ only depends on $\bar{y}$. This means that the orbit is not only symmetrical in the $\bar{x}$-axis, but also in the $\bar{y}$-axis. This gives the possibility to look only at the first quadrant of the periodic solution, from 0 to $\bar{\mathrm{X}}_h$ (see Figure 6.6).
With this information, the last integral (5.13) simplifies to

$$\mathrm{M}(h) = \pm 4 \int_0^{\bar{\mathrm{X}}_h} f(\bar{y}) d\bar{x}. \tag{6.14}$$

The sign is yet to be figured out. The direction of the integral with respect to $\bar{x}$ is known (the blue arrow), but with respect to t is yet to be determined. Using (6.12) and taking $\bar{x} > 0$ and $\bar{y} = 0$ as starting point of the periodic solution, we get $\dot{\bar{y}} = 2\bar{k_1}\bar{x}\left(\frac{\mu}{\sqrt{1+\bar{x}^2}} - 1\right)$, and because of $\bar{k_1} > 0$, $\bar{x} > 0$ and $\mu < 1$, it is found that $\dot{\bar{y}} < 0$. This means that the periodic orbit is negatively oriented (see the black arrows in Figure 6.6). Notice that in the first quadrant (marked) of the periodic solution, both integrals have the same direction. Therefore, the integral becomes

$$\mathrm{M}(h) = +4 \int_0^{\bar{\mathrm{X}}_h} f(\bar{y}) d\bar{x}. \tag{6.15}$$

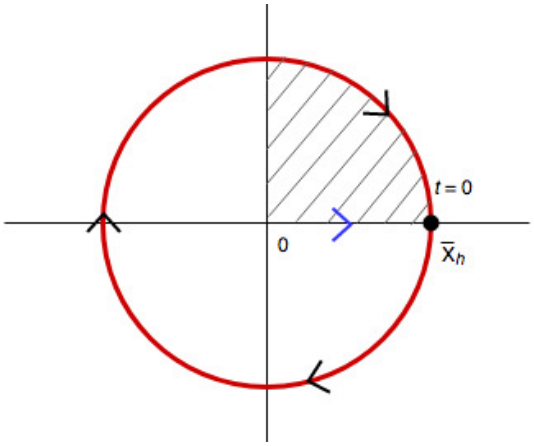

Figure 6.6: A periodic solution of (6.12). The orientation of (6.15) is indicated with the blue arrow and includes only the marked area. The orientation of the periodic solution is indicated with the black arrows.

The value of $\bar{X}_h$ is determined by $V(\bar{x}) = h$. Furthermore, $\bar{y}$ is determined by $H(\bar{x}, \bar{y}) = \frac{1}{2}\bar{y}^2 + V(\bar{x}) = h$, so $\bar{y} = \sqrt{2(h - V(\bar{x}))}$. This gives

$$M(h) = 4\int_0^{\bar{X}_h} f\left(\sqrt{2(h - V(\bar{x}))}\right) d\bar{x}. \tag{6.16}$$

This integral can be studied further:

$$M(h) = 4\int_0^{\bar{X}_h} f(\bar{y})d\bar{x} = 4\int_0^{\bar{X}_h} f(\sqrt{2(h - V(\bar{x}))})d\bar{x} \tag{6.17}$$

$$= 4\int_0^{\bar{X}_h} \sqrt{2(h - V(\bar{x}))}d\bar{x} - \frac{4}{3}\int_0^{\bar{X}_h} (2(h - V(\bar{x})))^{\frac{3}{2}}\, d\bar{x}. \tag{6.18}$$

We define the following:

$$I_1(h) = \int_0^{\bar{X}_h} \sqrt{2(h - V(\bar{x}))}d\bar{x} \tag{6.19}$$

$$= \int_0^{\bar{X}_h} \sqrt{2h + 2\bar{k_1}(2\mu\sqrt{1 + \bar{x}^2} - \bar{x}^2)}d\bar{x}, \tag{6.20}$$

$$I_2(h) = \int_0^{\bar{X}_h} (2(h - V(\bar{x})))^{\frac{3}{2}}\, d\bar{x} \tag{6.21}$$

$$= \int_0^{\bar{X}_h} \left(2h + 2\bar{k_1}(2\mu\sqrt{1 + \bar{x}^2} - \bar{x}^2)\right)^{\frac{3}{2}}\, d\bar{x}. \tag{6.22}$$

The Melnikov function can be rewritten as follows:

$$M(h) = 4I_1(h) - \frac{4}{3}I_2(h). \tag{6.23}$$

As stated before, the zeros of (6.23) resemble the existence of limit cycles. We seek the value of h for which $I(h) = 0$. We alter (6.23) in such a way that we can easily find $M(h) = 0$ numerically.

$$4I_1(h)\left(1 - \frac{I_2(h)}{3I_1(h)}\right) = 0. \tag{6.24}$$

We define $\mathrm{Q}(h) = \frac{\mathrm{I}_2(h)}{\mathrm{I}_1(h)}$ and search for the value(s) of h that give $\mathrm{Q}(h) = 3$. Then we know of the existence of a limit cycle. For a given value of h, $\bar{\mathrm{X}}_h$ follows from $V(\bar{\mathrm{X}}_h) = h$:

$$\bar{\mathrm{X}}_h = \pm\sqrt{\frac{h}{\bar{k_1}} + 2\mu^2 \pm 2\mu\sqrt{\mu^2 + \frac{h}{\bar{k_1}} + 1}}. \tag{6.25}$$

With this knowledge, (6.23) can be evaluated to find a limit cycle. This is done through a MATLAB script. The script can be found in Appendix C. It uses the Trapezium integration method to describe the integral of (6.23) against h, see Figure 6.8(a). The initial value of $\bar{y}$ is always set at 0, while the initial value for $\bar{x}$ varies. For this example, the parameters are chosen to be $\bar{k_1} = 1$ and $\mu = 0.5$. Figure 6.8(b) shows that the value for which $\mathrm{Q}(h) = 3$ and thus $\mathrm{I}(h) = 0$ equals $h = 0.95$. According to this figure, it seems to be the only value for which a limit cycle exists. Though $h = 0$ is a solution, it does not give a limit cycle. Evaluating $\mathrm{H}(\bar{x}, 0) = 0.95$ gives $\bar{x} = 1.71$.

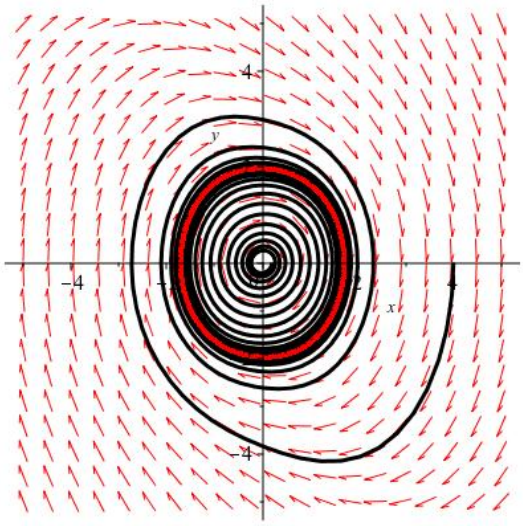

Figure 6.7: Phase portrait of (6.12) with $\bar{k_1} = 1$ and $\mu = 0.5$ with the stable limit cycle in red with value $h = 0.95$, with radius $\bar{x} = 1.71$ and curves at the interior (starting at $(\bar{x}, \bar{y}) = (0.2, 0)$) and exterior (starting at $(\bar{x}, \bar{y}) = (4, 0)$) of the solution, moving towards the limit cycle.

In Figure 6.7 it can be seen that the limit cycle indeed goes through $(1.71, 0)$. Curves starting outside of this cycle move towards the limit cycle, as do the curves starting inside of it, which indicates stability. This will be looked into more later on.
To make sure the MATLAB script is correct, it is applied to subproblem 1. This script can be found in Appendix B. We first need Melnikov's Function for this subproblem. This is found in the same way as for subproblem 2, which results in the following integral:

$$\mathrm{M}(h) = 4\int_0^{\bar{\mathrm{X}}_h} \sqrt{2h - \bar{k}\bar{x}^2}\,d\bar{x} - \frac{4}{3}\int_0^{\bar{\mathrm{X}}_h} \left(2h - \bar{k}\bar{x}^2\right)^{\frac{3}{2}}\,d\bar{x}. \tag{6.26}$$

The same definitions for $\mathrm{I}_1(h)$, $\mathrm{I}_2(h)$ and $\mathrm{Q}(h)$ hold. Again, using $V(\bar{\mathrm{X}}_h) = h$, we find $\bar{\mathrm{X}}_h = \sqrt{\frac{2h}{\bar{k}}}$. Finally, the results are shown in Figure 6.9. Just as in Section 6.1, we find $\mathrm{M}(2) = 0$ and $\mathrm{Q}(2) = 3$, so a limit cycle for $h = 2$. This validates the MATLAB script.

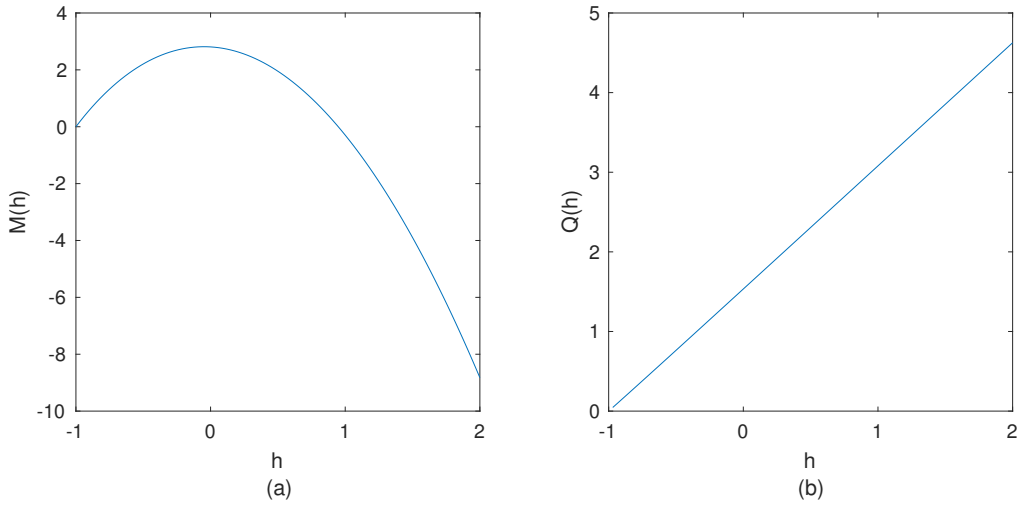

Figure 6.8: Value of Melnikov's Function (6.23) and value of Q(h) for different values of h, with $\bar{k_1} = 1$ and $\mu = 0.5$.

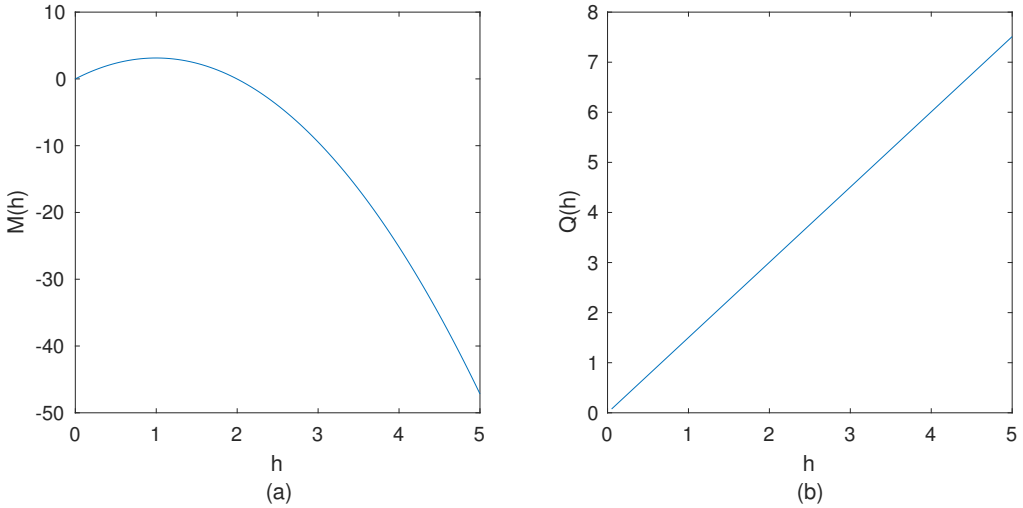

Figure 6.9: Value of (6.26) for subproblem 1 and value of Q(h) for different values of h, with $\bar{k} = 1$.

Now we know that there is one limit cycle and, for set parameter values, where its location is, we will determine its stability. We refer to the book of L. Perko [3], Chapter 4.10, Theorem 1. The theorem states that for set parameter values ($h, \bar{k_1}$ and μ) that give $M(h) = 0$, and $M_h(h) \neq 0$, the corresponding limit cycle is stable if $\varepsilon\omega_0 M_h(h) > 0$. ε is defined as a positive parameter in our problem, so we study the sign of $\omega_0 M_h(h)$. Therefore, we need to know the value of ω_0, which is equal to +1 when the corresponding periodic orbit is positively oriented and -1 when negatively oriented. We have seen in Figure 6.6 that the periodic solution is negatively oriented. All that is left to do now is check the sign of $M_h(h)$. This requires some more in-depth calculations.
The Melnikov function for this subproblem is as follows:

$$\mathrm{M}(h) = 4\int_0^{\bar{\mathrm{X}}_h} \sqrt{2h + 2\bar{k_1}(2\mu\sqrt{1+\bar{x}^2} - \bar{x}^2)}d\bar{x} - \frac{4}{3}\int_0^{\bar{\mathrm{X}}_h} \left(2h + 2\bar{k_1}(2\mu\sqrt{1+\bar{x}^2} - \bar{x}^2)\right)^{\frac{3}{2}} d\bar{x}. \tag{6.27}$$

The derivative of the Melnikov function with respect to h needs to be known. We define

$$w_1(h,\bar{x}) = \sqrt{2h + 2\bar{k_1}(2\mu\sqrt{1+\bar{x}^2} - \bar{x}^2)}, \tag{6.28}$$

$$w_2(h,\bar{x}) = \left(2h + 2\bar{k_1}(2\mu\sqrt{1+\bar{x}^2} - \bar{x}^2)\right)^{\frac{3}{2}}. \tag{6.29}$$

Remember the definition of $\bar{X}_h$ described in (6.25). In this subproblem, every $\pm$ in this expression gets a + sign. We get the following:

$$\frac{\partial \mathrm{M}}{\partial h}(h) = \frac{\partial}{\partial h}\left(4\int_0^{\bar{\mathrm{X}}_h} w_1 d\bar{x} - \frac{4}{3}\int_0^{\bar{\mathrm{X}}_h} w_2 d\bar{x}\right) \tag{6.30}$$

$$= 4\left(\int_0^{\bar{\mathrm{X}}_h} \frac{\partial w_1}{\partial h} d\bar{x} + w_1\left(h, \bar{\mathrm{X}}_h\right) \cdot \frac{\mathrm{d}\bar{\mathrm{X}}_h}{\mathrm{d}h} - w_1(h,0) \cdot \frac{\mathrm{d}0}{\mathrm{d}h}\right) \tag{6.31}$$

$$- \frac{4}{3}\left(\int_0^{\bar{\mathrm{X}}_h} \frac{\partial w_2}{\partial h} d\bar{x} + w_2\left(h, \bar{\mathrm{X}}_h\right) \cdot \frac{\mathrm{d}\bar{\mathrm{X}}_h}{\mathrm{d}h} - w_2(h,0) \cdot \frac{\mathrm{d}0}{\mathrm{d}h}\right) \tag{6.32}$$

$$= 4 \cdot \int_0^{\bar{\mathrm{X}}_h} \frac{1}{\sqrt{2h + 2\bar{k_1}(2\mu\sqrt{1+\bar{x}^2} - \bar{x}^2)}} d\bar{x} \tag{6.33}$$

$$+ \frac{4 \cdot w_1\left(h, \bar{\mathrm{X}}_h\right)}{2\sqrt{\frac{h}{\bar{k_1}} + 2\mu^2 + 2\mu\sqrt{\mu^2 + \frac{h}{\bar{k_1}} + 1}}} \cdot \left(\frac{1}{\bar{k_1}} + \frac{\mu}{\bar{k_1}\sqrt{\mu^2 + \frac{h}{\bar{k_1}} + 1}}\right) \tag{6.34}$$

$$- \frac{4}{3} \cdot \int_0^{\bar{\mathrm{X}}_h} 3\sqrt{2h + 2\bar{k_1}(2\mu\sqrt{1+\bar{x}^2} - \bar{x}^2)} d\bar{x} \tag{6.35}$$

$$- \frac{4 \cdot w_2\left(h, \bar{\mathrm{X}}_h\right)}{3 \cdot 2\sqrt{\frac{h}{\bar{k_1}} + 2\mu^2 + 2\mu\sqrt{\mu^2 + \frac{h}{\bar{k_1}} + 1}}} \cdot \left(\frac{1}{\bar{k_1}} + \frac{\mu}{\bar{k_1}\sqrt{\mu^2 + \frac{h}{\bar{k_1}} + 1}}\right). \tag{6.36}$$

We want to know $\mathrm{M}_h(h)$, with $h = 0.95$, $\bar{k_1} = 1$, $\mu = 0.5$ and $\bar{\mathrm{X}}_h = 1.71$, since for these parameters we find a limit cycle. Substituting these parameters in equation (6.30) gives -5.57. Since $\omega_0 = -1$ and $\mathrm{M}_h(h) = -5.57$, we find that $\omega_0 \mathrm{M}_h(h) > 0$ and thus, according to Theorem 1 of [3], the corresponding limit cycle is indeed stable.

6.2.2 Pressed in springs

Finally, subproblem 3 is examined. Remember the equation of motion and the Melnikov function for subproblem 2 respectively:

$$\ddot{\bar{x}} - 2\bar{k_1}\bar{x}\left(\frac{\mu}{\sqrt{1+\bar{x}^2}} - 1\right) = \varepsilon\left(\dot{\bar{x}} - \frac{1}{3}\dot{\bar{x}}^3\right), \tag{6.37}$$

$$\mathrm{M}(h) = 4\int_0^{\bar{\mathrm{X}}_h} \sqrt{2h + 2\bar{k_1}(2\mu\sqrt{1+\bar{x}^2} - \bar{x}^2)}d\bar{x} - \frac{4}{3}\int_0^{\bar{\mathrm{X}}_h} \left(2h + 2\bar{k_1}(2\mu\sqrt{1+\bar{x}^2} - \bar{x}^2)\right)^{\frac{3}{2}} d\bar{x}. \tag{6.38}$$

These stay mostly the same for subproblem 3, but there is one difference worth noting. For the case with stretched out springs, the assumption was made that the orbit $\mathrm{H}(\bar{x}, \bar{y}) = h$ was symmetrical in the $\bar{y}$-axis, but this is not necessarily the case for when the springs are pressed in. We will see two different situations, depending on the choice of parameters. First, we will look at $(\bar{k_1}, \mu) = (1, 1.5)$ and after that at $(\bar{k_1}, \mu) = (1, 3)$.

Outer limit cycle

For the limit cycle on the outside, the symmetry in the vertical axis still holds. The results for $(\bar{k_1}, \mu) = (1, 1.5)$ are shown in Figures 6.10 and 6.11(a). Figure 6.10 shows the results of the MATLAB script. It gives $h = -1.47$ and $\bar{\mathrm{X}}_h = 2.65$. This can also be seen in Figure 6.11(a). Figure 6.11(b) shows the phase portrait without wind.

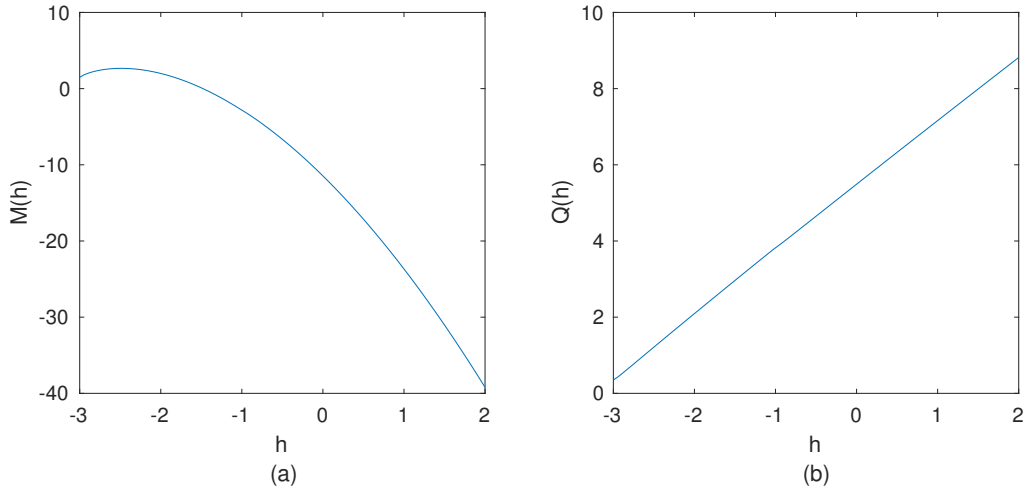

Figure 6.10: Value of Melnikov's Function (6.38) and value of $\mathrm{Q}(h)$ for different values of h, with $\bar{k_1} = 1$ and $\mu = 1.5$.

Using the same Theorem 1 from before from Perko [3], we find the same equation (6.30). The same reasoning as for subproblem 2 holds, since the periodic orbit is symmetrical in both the $\bar{x}$ and $\bar{y}$-axis and the Melnikov function goes from $\bar{x} = 0$ to $\bar{\mathrm{X}}_h$. We need to check if the periodic orbit is also negatively oriented for these parameters:

$$\dot{\bar{y}} = 2\bar{k_1}\bar{x}\left(\frac{\mu}{\sqrt{1+\bar{x}^2}} - 1\right) < 0, \tag{6.39}$$

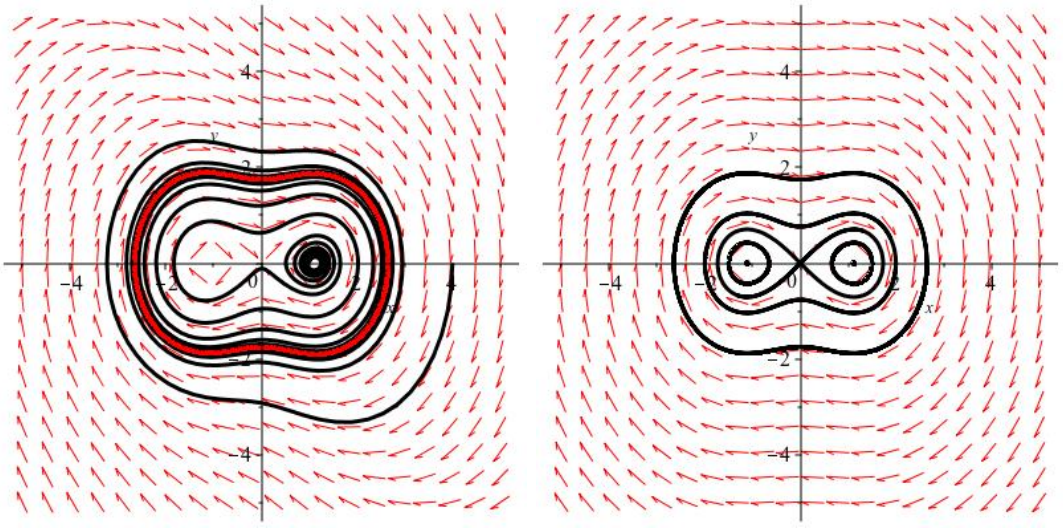

(a) (b)

Figure 6.11: (a) Phase portrait of (6.12) with $\bar{k_1} = 1$ and $\mu = 1.5$ with the stable limit cycle in red with value $h = -1.47$, at amplitude $\bar{x} = 2.65$ and curves at the interior (starting at $(\bar{x}, \bar{y}) = (1, 0)$) and exterior (starting at $(\bar{x}, \bar{y}) = (4, 0)$) of the solution, moving towards the limit cycle. (b) Phase portrait of (6.12) without any disturbance.

is true for $\mu = 1.5$ if $\bar{x} > \sqrt{1.25}$. Since the orbit starts at $t = 0$ in the location of $(\bar{\mathrm{X}}_h, \bar{y}) = (2.65, 0)$, this is indeed the case and $\omega_0 = -1$. Refer to Figure 6.12 to illustrate this. Substituting the new parameters gives us $\omega_0 \mathrm{M}_h(h) = 9.85 > 0$, thus is the limit cycle stable, which is also implied by Figure 6.11(a).

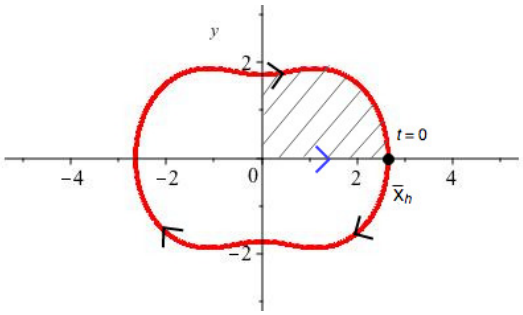

Figure 6.12: The periodic solution of (6.12) with $\bar{k_1} = 1$ and $\mu = 1.5$. The orientation of (6.38) is indicated with the blue arrow and includes only the marked area. The orientation of the periodic solution is indicated with the black arrows.

Inner limit cycles

As stated before, the limit cycles of this subproblem are not necessarily symmetrical in the vertical axis. For the parameter values $(\bar{k_1}, \mu) = (1, 3)$ we find two limit cycles, for which this is the case. The limit cycles themselves are not symmetric in their vertical axes, but they are mirrored in the $\bar{y}$-axis. For this reason, we cannot use the Melnikov function for only the first quadrant of the limit cycle. We call the starting point of the periodic orbit on the positive part of the $\bar{x}$-axis $t_\mathrm{R} = 0$, and on the negative part $t_\mathrm{L} = 0$. Referring to the Theory of Chapter 5, we find the following Melnikov functions for both periodic solutions:

$$\mathrm{M_R}(h) = 2\int_{\bar{\mathrm{X}}_{h1}}^{\bar{\mathrm{X}}_{h2}} \sqrt{2h + 2\bar{k_1}(2\mu\sqrt{1+\bar{x}^2} - \bar{x}^2)}d\bar{x} - \frac{2}{3}\int_{\bar{\mathrm{X}}_{h1}}^{\bar{\mathrm{X}}_{h2}} \left(2h + 2\bar{k_1}(2\mu\sqrt{1+\bar{x}^2} - \bar{x}^2)\right)^{\frac{3}{2}} d\bar{x}, \tag{6.40}$$

$$\mathrm{M_L}(h) = -2\int_{-\bar{\mathrm{X}}_{h1}}^{-\bar{\mathrm{X}}_{h2}} \sqrt{2h + 2\bar{k_1}(2\mu\sqrt{1+\bar{x}^2} - \bar{x}^2)}d\bar{x} + \frac{2}{3}\int_{-\bar{\mathrm{X}}_{h1}}^{-\bar{\mathrm{X}}_{h2}} \left(2h + 2\bar{k_1}(2\mu\sqrt{1+\bar{x}^2} - \bar{x}^2)\right)^{\frac{3}{2}} d\bar{x}. \tag{6.41}$$

The signs are based on the directions of the orientation of the periodic solution and the Melnikov function respectively, just as for the other subproblems. In Figure 6.13, it shows that the right orbit has a clockwise orientation, which is in the same direction as walking along the $\bar{x}$-axis from $\bar{\mathrm{X}}_{h1}$ to $\bar{\mathrm{X}}_{h2}$. The left limit cycle also has a clockwise orientation, but this is opposite from going from $-\bar{\mathrm{X}}_{h1}$ to $-\bar{\mathrm{X}}_{h2}$. Therefore, the Melnikov function $\mathrm{M_L}(h)$ gets a minus sign.

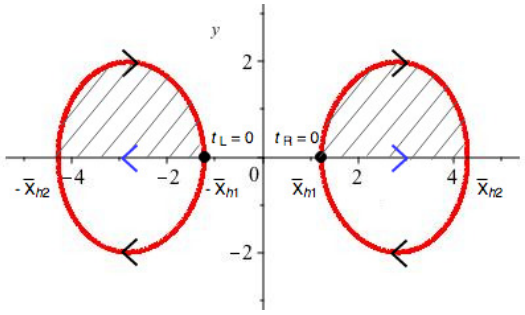

Figure 6.13: The periodic solution of (6.12) with $\bar{k_1} = 1$ and $\mu = 3$. The orientations of (6.40) and (6.41) are indicated with the blue arrows and include only the marked areas. The orientations of the periodic solutions are indicated with the black arrows.

It is also known that the two cycles are mirrored. Therefore, we will only need to study the stability of one of them and derive the stability of the other one. We study the cycle on the right side.

$$\frac{\partial \mathrm{M_R}}{\partial h}(h) = \frac{\partial}{\partial h}\left(2\int_{\bar{\mathrm{X}}_{h1}}^{\bar{\mathrm{X}}_{h2}} w_1 d\bar{x} - \frac{2}{3}\int_{\bar{\mathrm{X}}_{h1}}^{\bar{\mathrm{X}}_{h2}} w_2 d\bar{x}\right) \tag{6.42}$$

$$= 2\left(\int_{\bar{\mathrm{X}}_{h1}}^{\bar{\mathrm{X}}_{h2}} \frac{\partial w_1}{\partial h} d\bar{x} + w_1\left(h, \bar{\mathrm{X}}_{h2}\right) \cdot \frac{\mathrm{d}\bar{\mathrm{X}}_{h2}}{\mathrm{d}h} - w_1(h, \bar{\mathrm{X}}_{h1}) \cdot \frac{\mathrm{d}\bar{\mathrm{X}}_{h1}}{\mathrm{d}h}\right) \tag{6.43}$$

$$- \frac{2}{3}\left(\int_{\bar{\mathrm{X}}_{h1}}^{\bar{\mathrm{X}}_{h2}} \frac{\partial w_2}{\partial h} d\bar{x} + w_2\left(h, \bar{\mathrm{X}}_{h2}\right) \cdot \frac{\mathrm{d}\bar{\mathrm{X}}_{h2}}{\mathrm{d}h} - w_2(h, \bar{\mathrm{X}}_{h1}) \cdot \frac{\mathrm{d}\bar{\mathrm{X}}_{h1}}{\mathrm{d}h}\right). \tag{6.44}$$

Here, (6.28) and (6.29) still hold and we have

$$\bar{\mathrm{X}}_{h1} = \sqrt{\frac{h}{\bar{k_1}} + 2\mu^2 - 2\mu\sqrt{\mu^2 + \frac{h}{\bar{k_1}} + 1}}, \tag{6.45}$$

$$\bar{\mathrm{X}}_{h2} = \sqrt{\frac{h}{\bar{k_1}} + 2\mu^2 + 2\mu\sqrt{\mu^2 + \frac{h}{\bar{k_1}} + 1}}. \tag{6.46}$$

Because of the mirroring characteristics of the limit cycles, we get the following:

$$\mathrm{M_L}(h) = -2\int_{-\bar{\mathrm{X}}_{h1}}^{-\bar{\mathrm{X}}_{h2}} \sqrt{2h + 2\bar{k_1}(2\mu\sqrt{1+\bar{x}^2} - \bar{x}^2)}d\bar{x} + \frac{2}{3}\int_{-\bar{\mathrm{X}}_{h1}}^{-\bar{\mathrm{X}}_{h2}} \left(2h + 2\bar{k_1}(2\mu\sqrt{1+\bar{x}^2} - \bar{x}^2)\right)^{\frac{3}{2}} d\bar{x} \tag{6.47}$$

$$= 2\int_{\bar{\mathrm{X}}_{h1}}^{\bar{\mathrm{X}}_{h2}} \sqrt{2h + 2\bar{k_1}(2\mu\sqrt{1+\bar{x}^2} - \bar{x}^2)}d\bar{x} - \frac{2}{3}\int_{\bar{\mathrm{X}}_{h1}}^{\bar{\mathrm{X}}_{h2}} \left(2h + 2\bar{k_1}(2\mu\sqrt{1+\bar{x}^2} - \bar{x}^2)\right)^{\frac{3}{2}} d\bar{x} \tag{6.48}$$

$$= \mathrm{M_R}(h). \tag{6.49}$$

Before we can get any information from this, we need to determine the value of h for which $\mathrm{M_R} = \mathrm{M_L} = 0$ with $\bar{k_1} = 1$ and $\mu = 3$. The results can be seen in Figure 6.15 and are retrieved from the MATLAB script in Appendix D (which uses the left limit cycle for calculations). We find $h = -8.0$ and through this we find $\bar{\mathrm{X}}_{h1} = 1.23$ and $\bar{\mathrm{X}}_{h2} = 4.30$. This can be seen in Figure 6.14, both right and left.

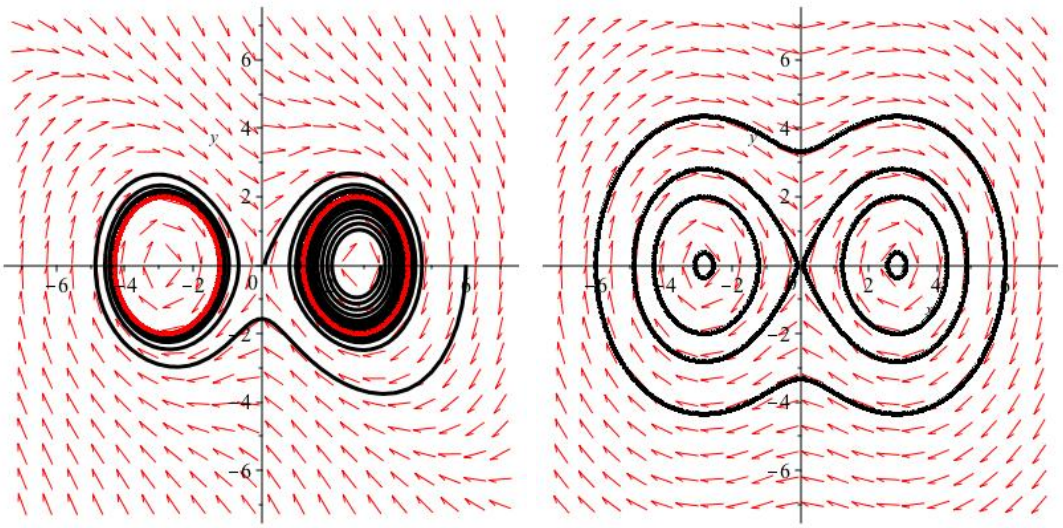

(a) (b)

Figure 6.14: (a) Phase portrait of (6.12) with $\bar{k_1} = 1$ and $\mu = 3$ with the stable limit cycles in red with value $h = -8.0$, at $\bar{\mathrm{X}}_{h1} = 1.23$ and $\bar{\mathrm{X}}_{h2} = 4.30$ and curves at the interior (starting at $(\bar{x}, \bar{y}) = (3.5, 0)$) and exterior (starting at $(\bar{x}, \bar{y}) = (0.1, 0)$ and $(6, 0)$) of the solution, moving towards one of the limit cycles. (b) Phase portrait of (6.12) without any disturbance.

Knowing the values of all parameters leads us to the last step. We can now establish the stability of the limit cycles. Substituting the values in Equation (6.42) and taking into account the negative orientation of the periodic orbits, we conclude the following: $\omega_0 \mathrm{M}_h(h) = 4.74 > 0$. This means that also these limit cycles are stable, which was implied by Figure 6.14(a).

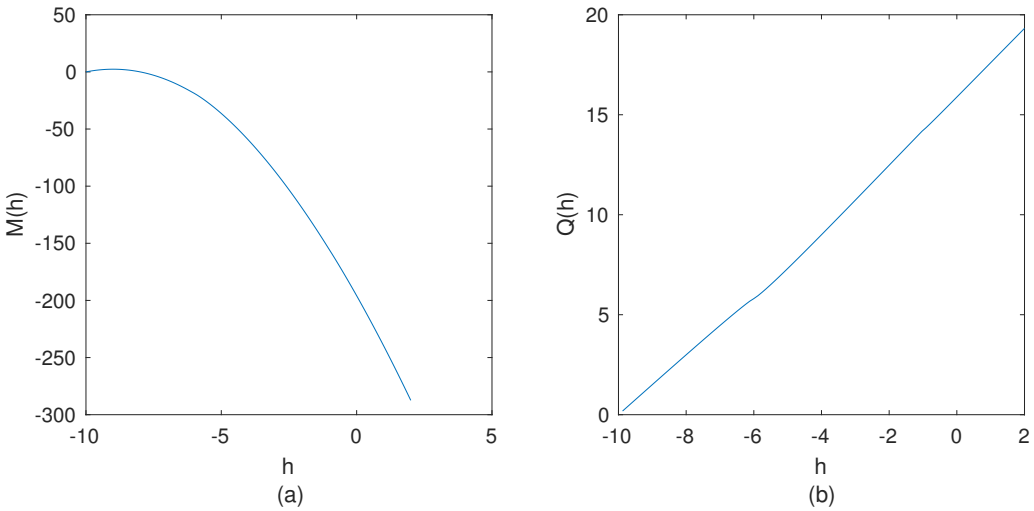

Figure 6.15: Value of Melnikov's Function (6.41) and value of Q(h) for different values of h, with $\bar{k_1} = 1$ and $\mu = 3$.

6.2.3 Three springs

For subproblem 4, Melnikov's Method can be applied to the complete equation of motion:

$$\ddot{\bar{x}} + \bar{k}\bar{x} - 2\bar{k_1}\bar{x}\left(\frac{\mu}{\sqrt{1+\bar{x}^2}} - 1\right) = \varepsilon\left(\dot{\bar{x}} - \frac{1}{3}\dot{\bar{x}}^3\right). \tag{6.50}$$

This will be left for later research.

7: Conclusions and Discussion

In this thesis, a mathematical model for a snap-through mass-spring system (Figure 7.1) was introduced. Equation of motion (7.1) was found for when a small disturbance, such as a wind force, acts on the mass.

$$\ddot{\bar{x}} + \bar{k}\bar{x} - 2\bar{k_1}\bar{x}\left(\frac{\mu}{\sqrt{1+\bar{x}^2}} - 1\right) = \varepsilon\left(\dot{\bar{x}} - \frac{1}{3}\dot{\bar{x}}^3\right). \tag{7.1}$$

It included several parameters to be tweaked: $\bar{k}$, $\bar{k_1}$ and μ. To be able to study the equation of motion, it was simplified and categorized into different subproblems, gradually increasing in their difficulty:

1. $\bar{k_1} = 0$
2. $\bar{k} = 0$, $0 < \mu \leq 1$
3. $\bar{k} = 0$, $\mu > 1$
4. $\bar{k_1}$, $\bar{k} \neq 0$

The first subproblem studies the case that only the vertical spring is attached to the mass. The second and third subproblems study the case that only the horizontal springs are attached, where subproblem 2 considers the springs to be stretched out and subproblem 3 considers them to be pressed in. Left for further research is subproblem 4, where all three springs are attached to the mass.

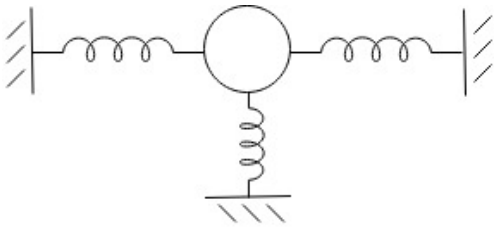

Figure 7.1: The mass-spring system with a snap-through mechanism.

Morse's Theorem was used to find behavioral characteristics for these different subproblems. The theory around Melnikov's Method was studied and applied to (7.1) for certain parameter values. Through this, we found limit cycles and their stability at certain locations that indicate the behavior of the mass in the mass-spring system when a wind force is acting on it. As far as possible, this was done algebraically. For more complex situations, a numerical model was set up.

The results show that for the first two subproblems, one stable limit cycle was found. The third subproblem, when the springs are initially pressed in, either has one stable limit cycle around

all equilibrium points, or two stable limit cycles, one around each centerpoint. Their amplitudes differ and they all describe a different motion. The fourth subproblem is yet to be studied.

There are multiple subjects in this thesis that could be looked into more. The numerical model is verified by applying it to the simplest problem, which was already analyzed algebraically. However, only the Trapezoidal method has been used for the analysis of the more complex subproblems. A program that uses Runge Kutta 4 on the system of differential equations from the more complex subproblems would ensure the results even more.

The plots that show the locations of the limit cycles ($Q(h)$ with respect to h) seem not to have multiple solutions. A way to prove this has not been found. This means that there might be limit cycles for multiple values of h, though it seems highly unlikely.

Most analyses are made to the general form of the equations, but some are applied to the equations with set parameter values. It would be an interesting study to look at what happens to the dynamical behavior of the system when tweaking these parameters $(\bar{k}, \bar{k_1}, \mu, \varepsilon)$. For example, there might be a situation with both the inner and outer cycles from subproblem 3.

The last and most complex subproblem has not been studied yet. This problem takes all defined parameters and components into account and thus describes reality best. Analyzing this would be the next step for further research.

References

[1] Brennan, M.J., Kovacic, I., Mace, B.R., Ramlan, R. (2010). Potential benefits of a non-linear stiffness in an energy harvesting device. Nonlinear Dynamics, 59, 545-558. https://doi.org./10.1007/s11071-009-9561-5

[2] Kooij, R.E., van Horssen, W.T. (1994). Bifurcation of Limit Cycles in a Particular Class of Quadratic Systems with Two Centres. Journal of Differential Equations, 114, 538-569.

[3] Perko, L. (2001). Differential Equations and Dynamical Systems (3). Flagstaff, USA: Springer.

[4] van Horssen, W.T. (1988). An asymptotic theory for a class of initial-boundary value problems for weakly nonlinear wave equations with an application to a model of the galloping oscillations of overhead transmission lines. Society for Industrial and Applied Mathematics, 48(6), 1234-1237.

[5] Verhulst, F. (1996). Nonlinear Differential Equations and Dynamical Systems (2). Berlin, Germany: Springer-Verlag.

Appendix

A Subproblem 1: Trapezoidal method on Equation 6.6

```
format bank

k = input('k = ');
n = 40;

s = 100;
h = linspace(0,5,s);

tbegin = 0;
tend = (2*pi)/sqrt(k);
t = linspace(tbegin,tend,n);
A1 = zeros(s,n);
for i = 1:s
    for j = 1:n-1
        A1(i,j) = (t(j+1)-t(j))*((I1(k,t(j),h(i))+I1(k,t(j+1),h(i)))
            /2);
    end
end

M = zeros(s,1);
for i=1:s
    M(i) = sum(A1(i,:));
end

plot(h,M);
xlabel({'h'})
ylabel({'M(h)'})

function I = I1(k,x,h)
    I = sqrt(2*h)*cos(sqrt(k)*x)*(sqrt(2*h)*cos(sqrt(k)*x)-1/3*(sqrt
        (2*h)*cos(sqrt(k)*x))^3);
end
```

B Subproblem 1: Trapezoidal method on the Melnikov Function

```
format bank
k = input('k = ');
n = 40;

s = 100;
h = linspace(0,5,s);

tbegin = 0;
tend = zeros(s,1);
t = zeros(s,n);
A1 = zeros(s,n);
A2 = zeros(s,n);
for i = 1:s
    tend(i) = sqrt(2*h(i)/k);
    t(i,:) = linspace(tbegin,tend(i),n);
    for j = 1:n-1
        A1(i,j) = real((t(i,j+1)-t(i,j))*((I1(k,t(i,j),h(i))+I1(k,t(i
            ,j+1),h(i)))/2));
        A2(i,j) = real((t(i,j+1)-t(i,j))*((I2(k,t(i,j),h(i))+I2(k,t(i
            ,j+1),h(i)))/2));
    end
end

B = zeros(s,2);
Q = zeros(s,1);
for i=1:s
    B(i,1) = sum(A1(i,:));
    B(i,2) = sum(A2(i,:));
    Q(i) = B(i,2)/B(i,1);
end

subplot(1,2,1);
plot(h,real(4*B(:,1)-4/3*B(:,2)))
xlabel({'h','(a)'})
ylabel({'M(h)'})
subplot(1,2,2);
plot(h,real(Q))
xlabel({'h','(b)'})
ylabel({'Q(h)'})

function I = I1(k,x,a)
    I = sqrt(2*a - k*x^2);
end
function I = I2(k,x,a)
    I = (sqrt(2*a - k*x^2))^3;
end
```

C Subproblem 2: Trapezoidal method on the Melnikov Function

```
format bank
k = input('k = ');
m = input('m = ');
n = 40;
s = 100;
h = linspace(-2*k*m,2,s);

tbegin = 0;
tend = zeros(s,1);
t = zeros(s,n);
A1 = zeros(s,n);
A2 = zeros(s,n);
for i = 1:s
    tend(i) = sqrt(h(i)/k + 2*m^2 + 2*m*sqrt(m^2 + h(i)/k + 1));
    t(i,:) = linspace(tbegin,tend(i),n);
    for j = 1:n-1
        A1(i,j) = real((t(i,j+1)-t(i,j))*((I1(k,m,t(i,j),h(i))+I1(k,m
            ,t(i,j+1),h(i)))/2));
        A2(i,j) = real((t(i,j+1)-t(i,j))*((I2(k,m,t(i,j),h(i))+I2(k,m
            ,t(i,j+1),h(i)))/2));
    end
end

B = zeros(s,2);
Q = zeros(s,1);
for i=1:s
    B(i,1) = sum(A1(i,:));
    B(i,2) = sum(A2(i,:));
    Q(i) = B(i,2)/B(i,1);
end

subplot(1,2,1);
plot(h,real(4*B(:,1)-4/3*B(:,2)))
xlabel({'h','(a)'})
ylabel({'M(h)'})
subplot(1,2,2);
plot(h,real(Q))
xlabel({'h','(b)'})
ylabel({'Q(h)'})

function I = I1(k,m,x,a)
    I = sqrt(2*a + 2*k*(2*m*sqrt(1 + x^2) - x^2));
end
function I = I2(k,m,x,a)
    I = (sqrt(2*a + 2*k*(2*m*sqrt(1 + x^2) - x^2)))^3;
end
```

D Subproblem 3: Trapezoidal method on the Melnikov Function

```
format bank
k = input('k = ');
m = input('m = ');
n = 40;
s = 100;
h = linspace(-2*k*m,2,s);

tbegin = zeros(s,1);
tend = zeros(s,1);
t = zeros(s,n);
A1 = zeros(s,n);
A2 = zeros(s,n);
for i = 1:s
    tbegin(i) = -(sqrt(h(i)/k + 2*m^2 - 2*m*sqrt(m^2 + h(i)/k + 1)));
    tend(i) = -(sqrt(h(i)/k + 2*m^2 + 2*m*sqrt(m^2 + h(i)/k + 1)));
    t(i,:) = linspace(tbegin(i),tend(i),n);
    for j = 1:n-1
        A1(i,j) = real((t(i,j+1)-t(i,j))*((I1(k,m,t(i,j),h(i))+I1(k,m
            ,t(i,j+1),h(i)))/2));
        A2(i,j) = real((t(i,j+1)-t(i,j))*((I2(k,m,t(i,j),h(i))+I2(k,m
            ,t(i,j+1),h(i)))/2));
    end
end

B = zeros(s,2);
Q = zeros(s,1);
for i=1:s
    B(i,1) = sum(A1(i,:));
    B(i,2) = sum(A2(i,:));
    Q(i) = B(i,2)/B(i,1);
end

subplot(1,2,1);
plot(h,real(-2*B(:,1)+2/3*B(:,2)))
xlabel({'h','(a)'})
ylabel({'M(h)'})
subplot(1,2,2);
plot(h,real(Q))
xlabel({'h','(b)'})
ylabel({'Q(h)'})

function I = I1(k,m,x,a)
    I = sqrt(2*a + 2*k*(2*m*sqrt(1 + x^2) - x^2));
end
function I = I2(k,m,x,a)
    I = (sqrt(2*a + 2*k*(2*m*sqrt(1 + x^2) - x^2)))^3;
end
```